Approximate 2DOF Digital Controller for Interleaved PFC Boost Converter

Yuto Adachi[1], Yohei Mochizuki[1], Kohji Higuchi[1], and Kosin Chamnongthai[2]

[1] The University of Electro-Communications 1-5-1,
Chofu-ga-oka, Chofu-shi, Tokyo 182-8585, Japan
adachi@francis.ee.uec.ac.jp, higuchi@ee.uec.ac.jp
[2] KMUTT, 126 Pracha-uthit Rd., Bangmond, Tungkru, Bangkok 10140, Thailand

Abstract. In recent years, improving of power factor and reducing harmonic distortion in electrical instruments are needed. In general, a current conduction mode boost converter is used for active PFC (Power Factor Correction). In a PFC boost converter, if a duty cycle, a load resistance and an input voltage are changed, the dynamic characteristics are varied greatly. This is the prime reason of difficulty of controlling the interleaved PFC boost converter. In this paper, the robust digital controller using an A2DOF (Approximate 2-Degree-Of-Freedom) method for suppressing the variation of output voltage in dynamic load response with high power factor and low harmonic is proposed. Experimental studies using a micro-processor for controller demonstrate that this type of digital controller is effective to improve power factor and to suppress output voltage variation.

Keywords: Power factor correction (PFC), Boost converter, Approximate 2DOF, Digital robust control, Micro-processor.

1 Introduction

In recent years, improving of power factor and reducing harmonic of power supply using nonlinear electrical instruments are needed. A passive filter and an active filter in AC lines are used for improving of the power factor and reducing the harmonic [1]. Generally a current conduction mode boost converter is used for an active PFC (Power Factor Correction) in electrical instruments. Especially, an interleaved PFC boost converter is used in order to make size compact, make efficiency high and make noise low. In the interleaved PFC boost converter, if a duty cycle, a load resistance and an input voltage are changed, the dynamic characteristics are varied greatly, that is, the interleaved PFC converter has non-linear characteristics. In many applications of the interleaved PFC converters, loads cannot be specified in advance, i.e., their amplitudes are suddenly changed from the zero to the maximum rating. This is the prime reason of difficulty of controlling the interleaved PFC boost converter.

Usually, a conventional Lag-Lead, an analog IC controller, a gain-scheduled controller designed to the approximated linear controlled object at one operating point is used for the PFC converter [2]. In the nonlinear interleaved PFC boost converter

I. Zelinka et al. (eds.), *AETA 2013: Recent Advances in Electrical Engineering and Related Sciences*, Lecture Notes in Electrical Engineering 282,
DOI: 10.1007/978-3-642-41968-3_15,

system, those controllers are not enough for attaining good performance [3]. In this paper, the robust controller for suppressing the change of step response characteristics and fluctuation of output voltage with high power factor and low harmonic is proposed. An approximate 2-degree-of-freedom (A2DOF) method [4] is applied to the interleaved PFC boost converter. The PFC converter is a nonlinear system and the models are changed at each operation point. The design and combining methods of two A2DOF controllers which can cope with nonlinear system or changing of the models with one controller is proposed. These two controllers are actually implemented on one microprocessor and connected to the PFC converter and the load. Experimental studies demonstrate that the digital controllers designed by proposed method satisfy the desired performances and are useful.

2 Interleaved PFC Boost Converter

2.1 Modeling of Interleaved Boost Converter

The interleaved PFC boost converter shown in Fig. 1 is manufactured.

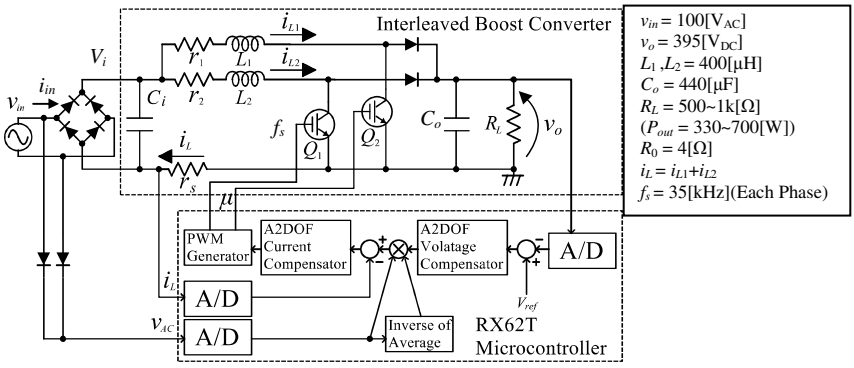

Fig. 1. Interleaved PFC boost converter

In Fig. 1, v_{in} is an input AC voltage, v_{AC} is an absolute value of the input AC voltage, i_{in} is an input AC current, C_i is a smoothing capacitor, V_i is a rectified and smoothed input voltage, and v_o is an output voltage. Q_1 and Q_2 are IGBTs, L_1 and L_2 are boost inductors, r_1 and r_2 are ESRs of inductors, D_1 and D_2 are diodes and i_L is the sum of inductor current, C_0 is an output capacitor. R_L is an output load resistance. The inductor current i_L is controlled to follow the rectified input voltage v_{AC} for improving power factor, reducing harmonics and stabilizing the output voltage. Using the state-space averaging method, the state equation of the interleaved boost converter becomes as follows [5]:

$$\frac{d}{dt}\begin{bmatrix} i_L \\ v_o \end{bmatrix} = \begin{bmatrix} -\dfrac{R_0}{L_0} & -\dfrac{1}{L_0} \\ \dfrac{1}{C_0} & -\dfrac{1}{R_L C_0} \end{bmatrix} \begin{bmatrix} i_L \\ v_o \end{bmatrix} + \begin{bmatrix} \dfrac{V_i}{L_0} \\ 0 \end{bmatrix} + \left\{ v_o \begin{bmatrix} \dfrac{1}{L_0} \\ 0 \end{bmatrix} + i_L \begin{bmatrix} 0 \\ -\dfrac{1}{C_0} \end{bmatrix} \right\} \mu \tag{1}$$

Here μ is duty cycle. When controlling the current of the sum of each phase, R_0 is $r_1r_2/(r_1+r_2)$ and L_0 is $L_1L_2/(L_1+L_2)$. The boost converter has non-linear characteristics because this equation has the product of state variable v_o, i_L and duty cycle μ.

2.2 Dynamic Characteristics of Boost Converter

At some operating point of eq. (1), let v_o, i_L and μ, be V_s, I_s and μ_s, respectively. Then the linear approximate state equation of the boost converter using small perturbations $\Delta i_L = i_L - I_s$, $\Delta v_o = v_o - V_s$ and $\Delta\mu = \mu - \mu_s$ is as follows:

$$\begin{aligned} \dot{x}(t) &= A_c x(t) + B_c u(t) \\ y(t) &= C_c x(t) \end{aligned} \tag{2}$$

where

$$A_c = \begin{bmatrix} -\dfrac{R_0}{L_0} & -\dfrac{1-\mu_s}{L_0} \\ \dfrac{1-\mu_s}{C_0} & -\dfrac{1}{R_L C_0} \end{bmatrix} \quad B_c = \begin{bmatrix} \dfrac{V_s}{L_0} \\ -\dfrac{I_s}{C_0} \end{bmatrix} \quad x(t) = \begin{bmatrix} \Delta i_L(t) \\ \Delta v_o(t) \end{bmatrix} \quad y = \begin{bmatrix} y_i \\ y_v \end{bmatrix} \quad u(t) = \Delta\mu(t) \quad C_c = \begin{bmatrix} 1 & 0 \end{bmatrix}$$

From this equation, matrix A_c and B_c of the boost converter depends on duty cycle μ_s. Therefore, the converter response will be changed depending on the operating point and other parameter variations. The changes of the load R_L, the duty cycle μ_s, the output voltage V_s and the inductor current I_s in the controlled object are considered as parameter changes. Such parameter changes can be replaced with the equivalent disturbances inputted to the input and the output of the controlled object. Therefore, what is necessary is just to constitute the control systems whose pulse transfer functions from equivalent disturbances to the output y become as small as possible in their amplitudes, in order to robustize or suppress the influence of these parameter changes.

3 Digital Robust Current Controller

3.1 Discretization of Controlled Object

The continuous system of eq. (2) is transformed into the discrete system as follows:

$$\begin{aligned} x(k+1) &= A_d x(k) + B_d u(k) \\ y(k) &= C_d x(k) \end{aligned} \tag{3}$$

where

$$A_d = \left[e^{A_c T}\right], B_d = \left[\int_0^T e^{A_c \tau} B_c d\tau\right], C_d = C_c$$

Here, in order to compensate the delay time by A/D conversion time and microprocessor operation time etc., one delay (state ξ_1) is introduced to input of the controlled object. Then the state-space equation is described as follows:

$$\begin{aligned} x_{dt}(k+1) &= A_{dt} x_{dt}(k) + B_{dt} v(k) \\ y(k) &= C_{dt} x_{dt}(k) \end{aligned} \tag{4}$$

where

$$A_{dt} = \begin{bmatrix} e^{A_c T_s} & e^{A_c (T_s - L_d)} \int_0^{L_d} e^{A_c \tau} B_c d\tau \\ 0 & 0 \end{bmatrix} = \begin{bmatrix} a_{11} & a_{12} & a_{13} \\ a_{21} & a_{22} & a_{23} \\ 0 & 0 & 0 \end{bmatrix}$$

$$B_{dt} = \begin{bmatrix} \int_0^{T_s - L_d} e^{A_c \tau} B_c d\tau \\ 1 \end{bmatrix} = \begin{bmatrix} b_{11} \\ b_{21} \\ 1 \end{bmatrix} \quad x_{dt}(k) = \begin{bmatrix} x(k) \\ \xi_1(k) \end{bmatrix} \quad C_{dt} = \begin{bmatrix} C_c & 0 \end{bmatrix} = \begin{bmatrix} 1 & 0 & 0 \end{bmatrix}$$

3.2 Design Method for A2DOF Digital Current Controller

The transfer function from the reference input r_i' to the output y_i is specified as follows:

$$W_{r_i' y i}(z) = \frac{(1+H_1)}{(z+H_1)} \frac{(1+H_2)}{(z+H_2)} \frac{(1+H_3)}{(z+H_3)} \frac{(z-n_{1i})}{(1-n_{1i})} \frac{(z-n_{2i})}{(1-n_{2i})} \tag{5}$$

Here H_i, i=1,2,3 are the specified arbitrary parameters, n_{1i} and n_{2i} are the zeros of the discrete-time controlled object. This target characteristic W_{ri}'$_{yi}$ is realizable by constituting the model matching system shown in Fig. 2 using the following state feedback to the controlled object.

$$v = -F x_{dt} - G_i r_i' \tag{6}$$

Here F = [f_1 f_2 f_3] and G_i are selected suitably. In Fig. 2 q_v and q_{yi} are the equivalent disturbances with which the parameter changes of the controlled object are replaced.

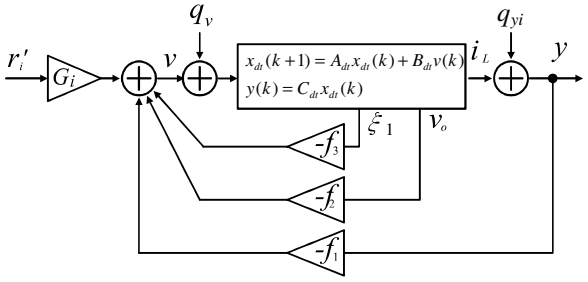

Fig. 2. Model matching system using state feedback

It shall be specified that the relation of H_1 and H_3 become $|H_1| >> |H_3|$ and $n_{1i} \approx H_2$. Then W_{ri}'$_{yi}$ can be approximated to the following first-order discrete-time model:

$$W_{r_i' y_i}(z) \approx W_{mi}(z) = \frac{1+H_1}{z+H_1} \tag{7}$$

The transfer function $W_{Qyi}(z)$ between the equivalent disturbance $Q_i = [q_v \; q_{yi}]^T$ to y_i of the system in Fig. 2 is defined as

$$W_{Qyi}(z) = [W_{qvyi}(z) \quad W_{qyyi}(z)] \tag{8}$$

The system added the inverse system and the filter to the system of Fig. 2 is constituted as shown in Fig. 3.

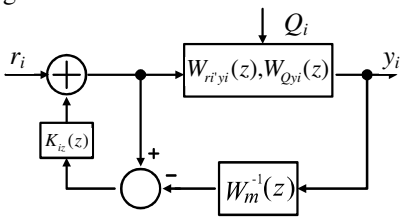

Fig. 3. System Reconstituted with Inverse System and Filter

In Fig. 3, the transfer function $K_i(z)$ is as follows:

$$K_i(z) = \frac{k_{zi}}{z-1+k_{zi}} \tag{9}$$

The transfer functions between r_i -y_i, q_{ui} -y_i and q_{yi} -y_i of the system in Fig. 3 are given by

$$y_i = \frac{1+H_1}{z+H_1} \frac{z-1+k_{zi}}{z-1+k_{zi}W_{si}(z)} W_{si}(z) r_i \tag{10}$$

$$y_i = \frac{z-1+k_{zi}}{z-1+k_{zi}} \frac{z-1+k_{zi}}{z-1+k_{zi}W_{si}(z)} W_{Qyi}(z) Q_i \tag{11}$$

where

$$W_{si}(z) = \frac{(1+H_3)(z-n_{1i})}{(z+H_3)(1-n_{1i})}$$

Here, if $W_{si}(z) \approx 1$, then eq. (10) and eq. (11) are approximated, respectively as follows:

$$y_i = \frac{1+H_1}{z+H_1} r_i \tag{12}$$

$$y_i = \frac{z-1}{z-1+k_{zi}} W_{Qyi}(z) Q_i \tag{13}$$

From eq. (12) and eq. (13), it turns out that the characteristics from r to y can be specified with H_1 and the characteristics from Q_i to y_i can be independently specified with k_{zi}. That is, the system in Fig. 3 is an A2DOF system, and its sensitivity against disturbances becomes lower with the increase of k_{zi}. If equivalent conversion of the controller in Fig. 3, we obtain Fig. 4. Then, substituting a system of Fig. 2 to Fig. 4, A2DOF digital integral type control system will be obtained as shown in Fig. 5. In Fig. 5, the parameters of the controller are as follows:

$$\begin{aligned} k_1 &= -f_1 - \frac{Gk_{zi}}{1+H_1}, \quad k_2 = -f_2 \\ k_3 &= -f_3, \quad k_{ii} = G_i k_{zi}, \quad k_{ri} = G_i \end{aligned} \tag{14}$$

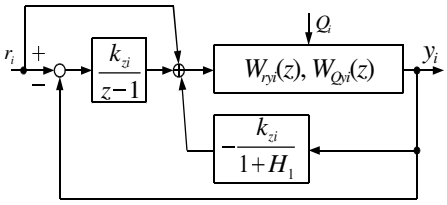

Fig. 4. Equivalent Conversion of the Robust Digital Controller

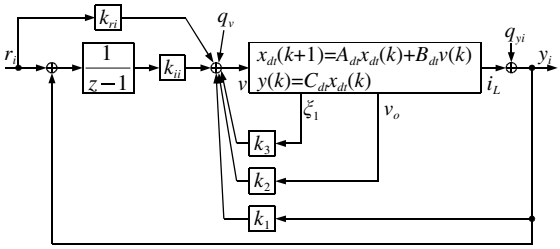

Fig. 5. Approximate 2DOF Digital Integral Type Current Control System

4 Digital Robust Voltage Controller

4.1 Addition of u_v and v_{ac} to r_i

Add the multiplier in front of the reference input ri of the current control system. Let the inputs of the multiplier be v_{ac} and u_v as shown in Fig. 6. In Fig. 6, v_{ac} is the absolute value of the input voltage v_{in} and u_v is a new input. This addition is for making the inductor current i_L follow the AC voltage v_{ac}.

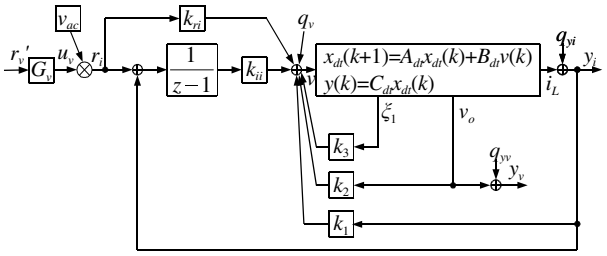

Fig. 6. Current Control System Added Multiplier

4.2 Approximate Controlled Object for Voltage Controller

The system of Fig. 6 becomes a controlled object for a voltage controller. Derive an approximated controlled object from this system for designing the voltage controller. In Fig. 6, u_v is a control input, and $v_o = y_v$ is an output of the controlled object. When u_v is set to0 $u_v = G_{vrv}$', the transfer function from r_v' to v_o is as follows:

$$v_o = \frac{(1+H_2)}{(z+H_2)}\frac{(1+H_1)}{(z+H_1)}\frac{(1+p_{1i})}{(z+p_{1i})}\frac{(1+p_{2i})}{(z+p_{2i})}\frac{(z-n_{1v})}{(1-n_{1v})}\frac{(z-n_{2v})}{(1-n_{2v})}r_v' = W_{ry_v}r_v' \tag{15}$$

where

$$G_v = \frac{1}{G_{uv}} = \frac{a_{21}+\frac{a_{23}}{G_{ui}}+\frac{b_{21}}{G_{ui}}}{1-a_{22}}, G_{ui} = \frac{1}{C_{dt}(I-A_{dt})^{-1}B_{dt}}$$

G_{uv} is DC gain between u_v to v_o. n_{1v}, n_{2v} are zeros of the transfer function from u_v to v_o.

In eq. (15) $|H_2|>>(|H_1|, |p_{1i}|, |p_{2i}|)$, so the controlled object W_{ryv} for the voltage controller is approximated as

$$W_{ry_v}(z) \approx W_{mv}(z) = \frac{1+H_2}{z+H_2} \tag{16}$$

4.3 Design Method of A2DOF Voltage Controller

The inverse system $W_{mv}^{-1}(z)$ and the filter $K_v(z)$ are added to the system of eq. (16) like Fig. 3. Here $K_v(z)$ is as follows:

$$K_v(z) = \frac{k_{zv}}{z-1+k_{zv}} \tag{17}$$

In Fig. 3, r_i, y_i, Q_i, q_v, q_{yi}, K_i, W_{ryi}, W_{mi}^{-1}, and W_{Qyi} are replaced with r_v, y_v, Q_v, q_v, q_{yv}, K_v, W_{ryv}, W_{mv}^{-1}, and W_{Qyv}, respectively. Then the transfer functions between r_v-y_v, q_v-y_v and q_{yv}-y_v of the system like Fig. 3 are given by

$$y_v \approx \frac{1+H_2}{z+H_2} r_v \tag{18}$$

$$y_v \approx \frac{z-1}{z-1+k_{zv}} W_{Q_v y_v}(z) Q_v \tag{19}$$

The A2DOF digital integral type control system will be obtained from the equivalent conversion of the controller like Fig. 4 as shown in Fig. 7.

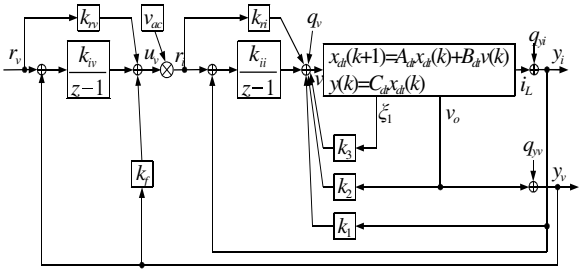

Fig. 7. Approximate 2DOF Digital Integral Type Control System Including the Current Controller and the Voltage Controller

In Fig. 7, the parameters of the voltage controller are as follows:

$$k_f = -\frac{G_v k_{zv}}{1+H_2} \quad k_{iv} = G_v k_{zv} \quad k_{rv} = G_v \tag{20}$$

5 Experimental Studies

All experimental setup system is shown in Fig. 8. A micro-controller (RX62T) from Renesas Electronics is used for the digital controller. Two digital controllers for the current and voltage were implemented on one Micro Controller.

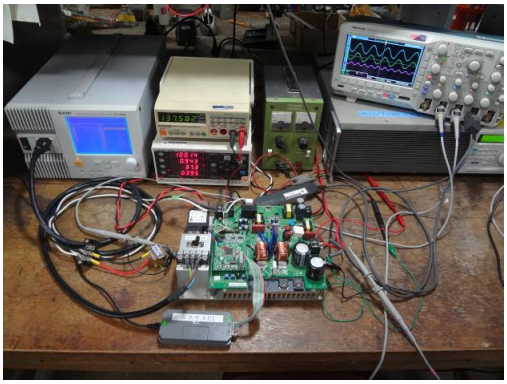

Fig. 8. Experimental setup system

In this experiment, the sampling frequency is $2f_s$ (f_s is a switching frequency) and the design parameters are set up as follows.

$H_1 = -0.8$ $H_2 = -0.9988$ $H_3 = -0.1$ $k_{zi} = 0.04$ $k_{zv} = 0.85$

From eq. (14) and eq. (20), the controller parameters are obtained as follows.

$k_1 = -0.0139755$ $k_2 = 0.000139848$ $k_3 = 0.0476263$
$k_{ii} = 0.0024912$ $k_{ri} = 0.06228$ $k_f = -5.70004$
$k_{iv} = 0.00684005$ $k_{rv} = 0.00804711$

The experiment result of the steady state using the proposed controller is shown in Fig. 9. The input current waveform and the phase are almost same as the input voltage, and the power factor at 500[Ω](300[W]) is 0.983. The experimental result of the steady state using the conventional digital Lag-Lead controller is shown in Fig. 10. The input current waveform is distorted more than the one in Fig. 9. at the zero cross point. That is, the proposed controller can reduce harmonics. The experimental result of dynamic load response using the proposed controller and the conventional digital Lag-Lead controller are shown in Fig. 11 and Fig.12, respectively. The output voltage fluctuations in dynamic load response of both results are less than 9[V](2.5[%] of vo), but the oscillation is not seen in the result of the proposed method. It turns out that proposed method is better than the conventional method in the performance of the output regulation in dynamic load response.

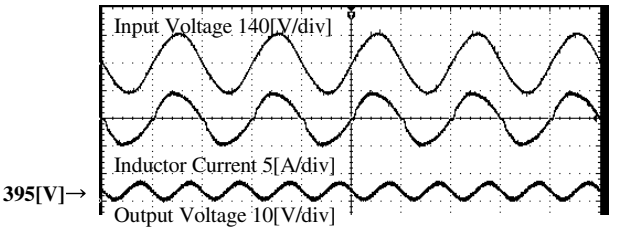

Fig. 9. Experimental Results of Steady State Waveforms using of the proposed A2DOF current and voltage controller PF = 0.98 (x-axis 10[ms/div])

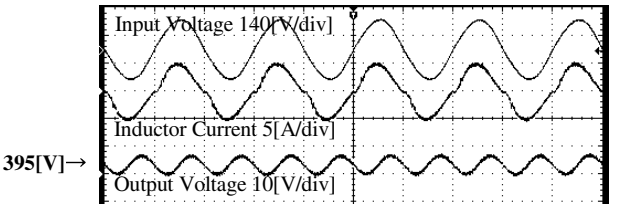

Fig. 10. Experimental Results of Steady State Waveforms using of the conventional Lag-Lead controller PF = 0.98 (x-axis 10[ms/div])

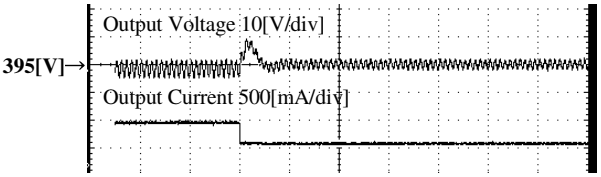

Fig. 11. Experimental Results of dynamic load response R_L = 1000[Ω] to 500[Ω] using of the proposed A2DOF current and voltage controller (x-axis 100[ms/div])

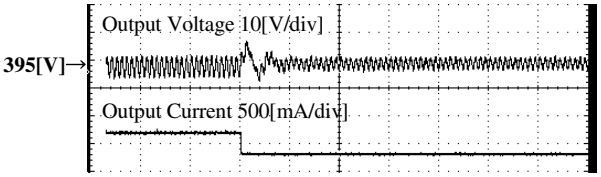

Fig. 12. Experimental Results of dynamic load response R_L = 1000[Ω] to 500[Ω] using of the conventional Lag-Lead controller (x-axis 100[ms/div])

6 Conclusion

In this paper, the concept of the digital controller which attains good robustness for the interleaved PFC boost converter was given. The proposed digital controller was implemented on the micro-processor. The PFC boost converter built-in this micro-processor was manufactured. It was shown from experiments that the digital controller which combined two A2DOF can suppress the output voltage variations in dynamic load response while attaining the high power factor and the low harmonic. This fact demonstrates the usefulness and practicality of our proposed method. A future subject is checking experimentally the change of the output voltage when the input voltage is changed.

References

1. Rossetto, L., Spiazzi, G., Tenti, P.: Control Techniques for Power Factor Correction Converters. In: Proc. PEMC 1994, pp. 1310–1318 (1994)
2. Zhang, W., Feng, G., Liu, Y., Wu, B.: A Digital Power Factor Correction (PFC) Control Strategy Optimized for DSP. IEEE Transactions on Power Electronics 19(6), 1474–1485 (2004)
3. Figueres, E., Benavent, J.M., Garcera, G., Pascual, M.: A Control Circuit With Load-Current Injection for Single-Phase Power-Factor-Correction Rectifiers. IEEE Transactions on Industrial Electronics 54(3), 1272–1281 (2007)
4. Higuchi, K., Nakano, K., Kajikawa, T., Takegami, E., Tomioka, S., Watanabe, K.: A New Design of Robust Digital Controller for DC-DC Converters. In: IFAC 16th Triennial World Congress, CD-ROM (2005)
5. Sasaki, S., Watanabe, H.: Analysis of Multiple Operating Points for Dynamical Control of Switching Power Converters. IEIC Technical Report, pp. 33–38 (2005)